

# Parameterization of the LHCb Magnetic Field Map

A. Keune<sup>a</sup>

for the LHCb collaboration

<sup>a</sup>Ecole Polytechnique Fédérale de Lausanne, Switzerland

A parameterization of the LHCb magnetic field is presented. It is derived from an analysis of data from a high-precision survey in and around the 4 Tm dipole magnet. By optimally using both data measurements and simulation values, a precision of less than  $10^{-3}$  Tesla is achieved for the two polarities.

The LHCb detector at the Large Hadron Collider is a single arm spectrometer with an acceptance region of 300 mrad in horizontal ( $x$ ) and 250 mrad in vertical ( $y$ ) direction. A 4 Tm dipole magnet ensures particle separation and enables momentum measurements, with the  $xz$ -plane as its main bending plane. The magnetic field parameterization is a realistic description based on data measurements and covers the full acceptance region. Two polarities, upward (upward  $B_y$ -component) and downward (downward  $B_y$ -component), are used to determine systematic tracking errors. Following on from [1], the analysis is developed for the upward polarity and applied without further tuning to the downward polarity. As  $B_y$  is the main field component, its results are stressed.

## 1. Magnetic Field Measurements

Magnetic field measurements were taken in December 2005 using sensors containing three orthogonal Hall probes [2]. Sixty sensors were distributed on two adjacent plates, separated by 64 mm, over a grid of  $80 \times 80$  mm<sup>2</sup>. These plates were placed orthogonally to the  $z$ -axis and adjustable in steps of 80 mm in both  $x$  and  $y$  direction and in steps of 100 mm in  $z$  direction. The design thus provides overlapping measurements used to crosscheck the data. All visibly non-physical and inconsistent measurements are removed from the data set. For both upward and downward polarity less than 5% of measurements are removed, resulting in  $\sim 280$ k upward polarity measurements and  $\sim 215$ k downward polarity measurements, of

which  $\sim 260$ k and  $\sim 202$ k lie within the acceptance region, respectively. However, due to a then partially commissioned detector and limited reach of the equipment, these measurements do not cover the full acceptance region.

Of all the measurements  $\sim 60$ k ( $B_y > 0$ ) and  $\sim 48$ k ( $B_y < 0$ ) overlap. Additionally  $\sim 289$ k measurements recorded the magnetic field at the same coordinate for both polarities. The results of the overlapping measurements are given in Table 1 and for the both-polarity comparison in Table 2. Using these data, the measurement error is estimated to be less than  $10^{-3}$  Tesla. As expected, the error decreases as more data is used. In addition, the large  $B_z$  discrepancies, which dominated the result based on overlapping measurements, solely result in a large shoulder in the both-polarity comparison. In addition,  $\delta B_y$ , the difference in field size of the  $B_y$ -component, is depicted in Figures 1 and 2 together with the corresponding single Gaussian fits.

Table 1  
Measurement errors (T) based on overlapping measurements for both polarities.

	upward	downward
$B_x$	$1.0 \cdot 10^{-3}$	$8.2 \cdot 10^{-4}$
$B_y$	$1.0 \cdot 10^{-3}$	$8.0 \cdot 10^{-4}$
$B_z$	$2.4 \cdot 10^{-3}$	$9.5 \cdot 10^{-4}$
Magnitude	$5.1 \cdot 10^{-4}$	$3.7 \cdot 10^{-4}$

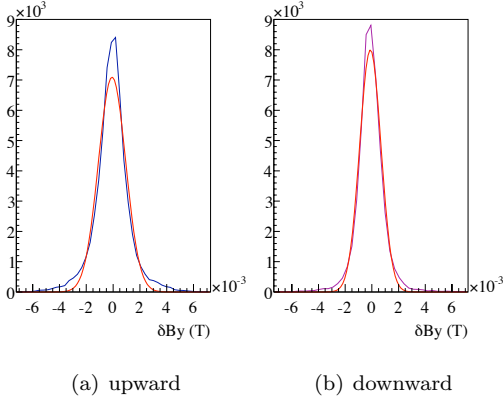


Figure 1.  $\delta B_y$  (T) of same coordinate measurements for (a) upward and (b) downward polarity, plus corresponding Gaussian fits.

Table 2

Measurement errors (T) based on the addition of up- and downward polarization measurements.

(upward polarity)+(downward polarity)	
$B_x$	$4.4 \cdot 10^{-4}$
$B_y$	$3.6 \cdot 10^{-4}$
$B_z$	$3.4 \cdot 10^{-4}$ (large shoulder)
Magnitude	$3.0 \cdot 10^{-4}$

## 2. Simulation and Extrapolation

For the parameterization of the magnetic field high power polynomials are needed to accurately describe the field. Because the data measurements do not cover the full acceptance region of the detector, extrapolation is used to determine the field in these areas. However, high order polynomials induce large errors when extrapolated. To minimize this effect the differences between the data measurements and the simulation values are parameterized instead of the data measurements themselves. These differences are smooth, continuous functions which fluctuate less and extrapolate in a more controlled manner.

A simulated magnetic field map is available over the full acceptance of the detector. Simulation values are calculated using the finite element model TOSCA [2,3] and are interpolated to a grid of  $100 \times 100 \times 100 \text{ mm}^3$  within the applica-

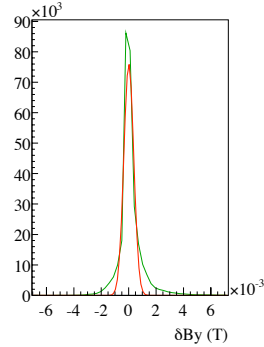


Figure 2.  $\delta B_y$  (T) of same coordinate measurements for (upward polarity)+(downward polarity) data, plus corresponding Gaussian fits.

tion. These values are interpolated to match the coordinates of the data measurements.

## 3. Fitting Method

A 3D polynomial fit is applied to the differences between measurements and simulation. This fit is predefined in ROOT as TMultiDimFit [4], intended for complex 3D parameterizations. The option of Chebyshev polynomials is chosen to perform the fit. Restricting the maximum order of the polynomials per dimension to either 3 or 4 is sufficient to ensure accurate results, yet controlled extrapolation.

The parameterization is divided up in areas of different  $z$ -coordinate. The divisions are based on fluctuations in differences between measurement and simulation and are later fine-tuned after visual inspection of the fitting. In total the data measurements are divided into 11 regions, ranging from  $z = -0.5 \text{ m}$  to  $z = 9.1 \text{ m}$  where  $z = 0 \text{ m}$  is the interaction point and the magnet region extends from  $z = 3 \text{ m}$  to almost  $z = 8 \text{ m}$ . A small overlap between the fitting regions ensures that discrepancies on the boundaries between areas are of the order of the fit error, as shown in Table 3 and Figure 3.

Data measurements outside the acceptance region are only used in the upstream region. Adding these measurements to the small number of data measurements within the upstream acceptance region improves the fit results. The mea-

measurements outside the magnet and downstream acceptance region are not included in the fit as the magnetic field shape of the simulation is not continuous throughout this region and in addition the added complexity of the differences makes the fit inside the acceptance region less accurate.

The data measurements are taken up to  $z = 9.1$  m, but an accurate parameterization needs to be derived over the full acceptance region, extending up to  $z = 14$  m. Extrapolation is not relied upon to give reasonable values. Instead, the differences between simulation and data measurement are taken at  $z = 9$  m, where the fit is still very accurate, and are reduced as a function of  $z$  to follow the shape obtained from the simulation as it eventually reduces to zero.

To control the parameterization outside the acceptance region, the difference between data and simulation is taken at the closest point within the acceptance region. This is done to satisfy the software requirement of a full grid up to  $x$ - and  $y$ -coordinates of 4000 mm for all  $z$ -coordinates.

#### 4. Parameterization Results

Fitting residuals are of the order of  $10^{-3}$  T. The simulated values are interpolated onto the coordinates of the data measurements by selecting for each measurement a cube of  $300 \times 300 \times 300$  mm<sup>3</sup>, containing 27 simulation values and using the same 3D fitting method to determine accurate simulation values. Although it is difficult to estimate an error, the fitting residuals differ by a few  $10^{-5}$  T, depending on the chosen interpolation method. The residuals of the parameterization are given in Table 4 and depicted for the  $B_y$ -component in Figure 4.

#### 5. Polarity Comparison

Differences in parameterization between upward and downward polarity are under  $10^{-3}$  T. Keeping in mind that these results are based on  $\sim 81k$  data points ( $z \leq 9.1$  m) the obtained errors are satisfactory. The results are shown in Table 5 and depicted for the  $B_y$ -component in Figure 5.

Table 3

$\delta B_y$  (T) discrepancies at the boundaries of two fit areas.

upward polarity	
$B_x$	$(-0.8 \pm 2.7) \cdot 10^{-4}$
$B_y$	$(1.7 \pm 4.1) \cdot 10^{-4}$
$B_z$	$(0.6 \pm 5.2) \cdot 10^{-4}$
downward polarity	
$B_x$	$(0.7 \pm 4.0) \cdot 10^{-4}$
$B_y$	$(-0.6 \pm 4.2) \cdot 10^{-4}$
$B_z$	$(0.2 \pm 7.4) \cdot 10^{-4}$

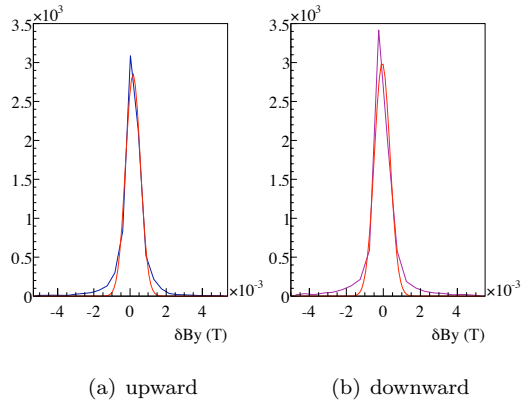


Figure 3.  $\delta B_y$  (T) discrepancies at the boundaries of two fit areas, plus corresponding Gaussian fits.

#### 6. Integrated Field

The LHCb integrated field,  $\int B \cdot dl$ , is  $\sim 4$  Tm when integrated over the detector length in  $z$ -direction. With the  $xz$ -plane the main bending plane,  $Bdl_x$  is the main contributing component. From the interaction point, the magnetic field is integrated over straight paths, with slopes  $t_x$  and  $t_y$  ranging between  $[-0.3, 0.3]$  rad and  $[-0.25, 0.25]$  rad respectively, matching the acceptance region.  $Bdl_x$  as a function of the slope  $t_x$  in  $x$ -direction is depicted in Figure 6 for the upward and downward parameterizations as well as for the simulation values. The integrated field of the simulation values is significantly higher than those using either the (flipped-sign) upward or downward parameterization, which show similar results.

Table 4  
Residuals (T) of upward and downward polarity parameterizations.

	upward	downward
$B_x$	$8.7 \cdot 10^{-4}$	$7.7 \cdot 10^{-4}$
$B_y$	$8.1 \cdot 10^{-4}$	$6.6 \cdot 10^{-4}$
$B_z$	$1.7 \cdot 10^{-3}$	$1.1 \cdot 10^{-3}$
Magnitude	$7.9 \cdot 10^{-4}$	$5.4 \cdot 10^{-4}$

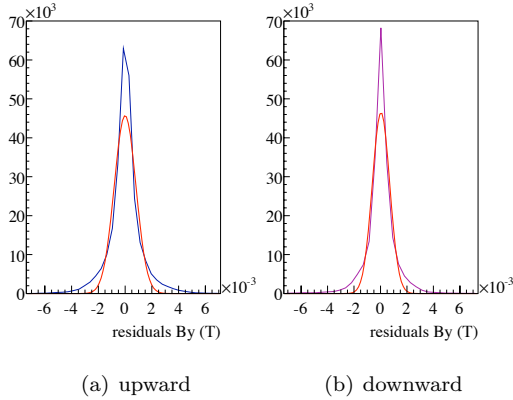


Figure 4.  $B_y$  residuals (T) for (a) upward and (b) downward polarity, plus corresponding Gaussian fits.

Table 5  
Residuals between up- and downward polarization (T).  $z \leq 9.1$  m.

(upward polarity)+(downward polarity)	
$B_x$	$7.2 \cdot 10^{-4}$
$B_y$	$5.4 \cdot 10^{-4}$
$B_z$	$5.5 \cdot 10^{-4}$
Magnitude	$5.4 \cdot 10^{-4}$

## 7. Conclusion

A parameterization of the LHCb magnetic field has been prepared for both polarities of the dipole field. This parameterization and the original measurements are accurate to  $\sim$ mT. In 2009 this parameterization will be used in the reconstruction of charged particle tracks when, for the first time the LHCb magnet is powered in the presence

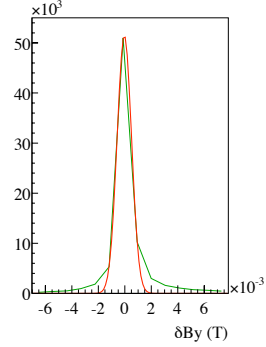


Figure 5.  $\delta B_y$  (T) of same coordinate fitting results for (upward polarity)+(downward polarity), plus corresponding Gaussian fits.

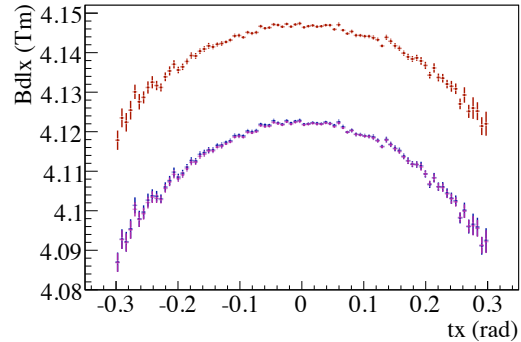


Figure 6. The integrated field component  $Bdl_x$  (Tm) vs  $t_x$  (rad) derived by using simulation (red, top curve) and upward (blue) and downward (magenta) parameterization (bottom curves).

of LHC collisions.

## REFERENCES

1. Parameterization of the LHCb Magnetic Field Map, G. Conti and A. Hicheur, Nuclear Science Symposium Conference Record, 2007. NSS '07. IEEE. Volume 4, pages 2439-2443.
2. Tests and Field Map of LHCb Dipole Magnet, M.Losasso et al., IEEE Transactions on Applied Superconductivity, Volume 16, Issue 2, pages 1700-1703, June 2006.
3. [www.vectorfields.com](http://www.vectorfields.com)
4. [root.cern.ch/root/html/TMultiDimFit.html](http://root.cern.ch/root/html/TMultiDimFit.html)